Bioorganic & Medicinal Chemistry 18 (2010) 5519–5527

Contents lists available at ScienceDirect

Bioorganic & Medicinal Chemistry

journal homepage: www.elsevier.com/locate/bmc

# Pharmacophore identification, synthesis, and biological evaluation of carboxylated chalcone derivatives as $CysLT_1$ antagonists

Xiaowu Dong [a], Li Wang [a], Xueqin Huang [b], Tao Liu [a], Erqing Wei [b], Lilin Du [a], Bo Yang [c], Yongzhou Hu [a,*]

[a] ZJU-ENS Joint Laboratory of Medicinal Chemistry, College of Pharmaceutical Sciences, Zhejiang University, Hangzhou 310058, China
[b] Department of Pharmacology, School of Medicine, Zhejiang University, Hangzhou 310058, China
[c] Institute of Pharmacology & Toxicology, College of Pharmaceutical Sciences, Zhejiang University, Hangzhou 310058, China

ARTICLE INFO

*Article history:*
Received 22 April 2010
Revised 12 June 2010
Accepted 15 June 2010
Available online 20 June 2010

*Keywords:*
$CysLT_1$ antagonists
HypoGen
Pharmacophore model
Carboxylated chalcone
QSAR

ABSTRACT

The pharmacophore model (Hypo1) with a well prediction capacity for $CysLT_1$ antagonists was developed using Catalyst/HypoGen program. Virtual screening against an in-house database consisted of carboxylated chalcones using Hypo1 was performed. Retrieved hits **26a**, **26b**, **27a**, and **27b** were synthesized and biological evaluated, the results of which demonstrated that these compounds showed moderate to good $CysLT_1$ antagonistic activities. This study indicated that the generated model (Hypo1) is a reliable and useful tool in lead optimization for novel $CysLT_1$ antagonists.



## 1. Introduction

Peptidoleukotrienes ($LTC_4$, $LTD_4$, $LTE_4$), also referred as cysteine-containing leukotrienes (Cys-LTs), play crucial roles in respiratory diseases (such as asthma and allergic rhinitis)[1–3] and other inflammatory conditions including cardiovascular, gastrointestinal and immune disorders.[4–6] The biological action of peptidoleukotrienes can be modulated by intervening biosynthesis or blocking the $CysLT_1$ receptor, which belongs to the G-protein-coupled receptors (GPCR) superfamily.[7–10]

Extensive studies on $CysLT_1$ antagonists have led to the discovery of a wide range of compounds (Fig. 1), such as indoles (e.g., Zafirlukast),[11] benzamides (e.g., Pranlukast)[12] and quinolines (Montelukast).[13] Important structural features for high potency were concluded from these reported $CysLT_1$ antagonists:[14] (i) a lipophilic anchor, which fits into the lipophilic pocket of the $CysLT_1$ receptor; (ii) a central flat unit, which mimics the triene system of the natural agonist $LTD_4$; (iii) one or two acidic groups, which resembles the peptide unit and/or the C1-carboxylic acid of $LTD_4$. Since the X-ray crystal structure of $CysLT_1$ receptor is not available, ligand-based modeling studies including 3D-QSAR models have been widely performed. Terada et al. proposed a 3D-QSAR model based on the comparison of Pranlukast and some derivatives with $LTE_4$ and proposed the activation site of the $CysLT_1$ receptor.[15] Palomer et al. established two 3D-QSAR models based on series of quinolines-based $CysLT_1$ antagonists which may act in a similar preferential fashion.[16] However, none of the QSAR models proposed so far was applied in virtual screen for novel $CysLT_1$ antagonists.

In this study, a pharmacophore-based lead optimization protocol was applied to discover novel potent $CysLT_1$ antagonists. At first, a novel 3D pharmacophore model was proposed based on different $CysLT_1$ antagonists using Catalyst/HypoGen program (Catalyst 4.1, Molecular Simulations Inc, San Diego, CA). Then, pharmacophore-based virtual screen was performed to search an in-house database consisted of newly designed carboxylated chalcones according to the literatures.[17] Furthermore, preferable screened hits were picked up, synthesized and biological evaluated to validate the reliability of the obtained pharmacophore model.

## 2. Computational methods

### 2.1. Data preparation

For the pharmacophore modeling studies, a set of 77 $CysLT_1$ antagonists were selected from the literatures,[16–21] and divided into a training set (25 molecules, Fig. 2) and a test set (52 molecules, Fig. S1, Supplementary data) based on principles of structural diversity and wide coverage of the activity range (between 0.19 and 55,000 nM). Besides, the 1500 negatives compounds used in enrichment studies were retrieved from Available

* Corresponding author. Tel./fax: +86 571 888208460.
*E-mail address:* huyz@zju.edu.cn (Y. Hu).

0968-0896/$ - see front matter © 2010 Elsevier Ltd. All rights reserved.
doi:10.1016/j.bmc.2010.06.047

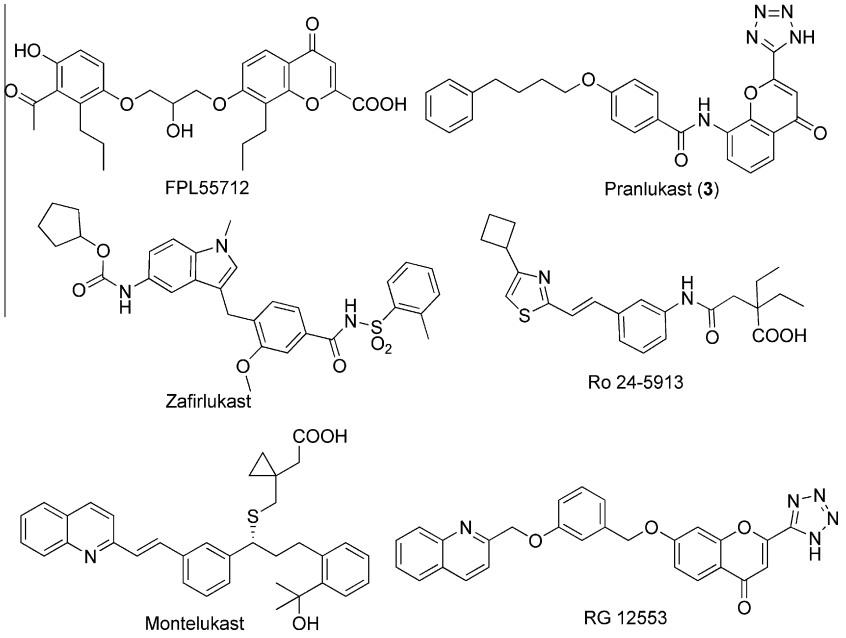


**Figure 1.** The 2D structures of some typical $CysLT_1$ antagonists.

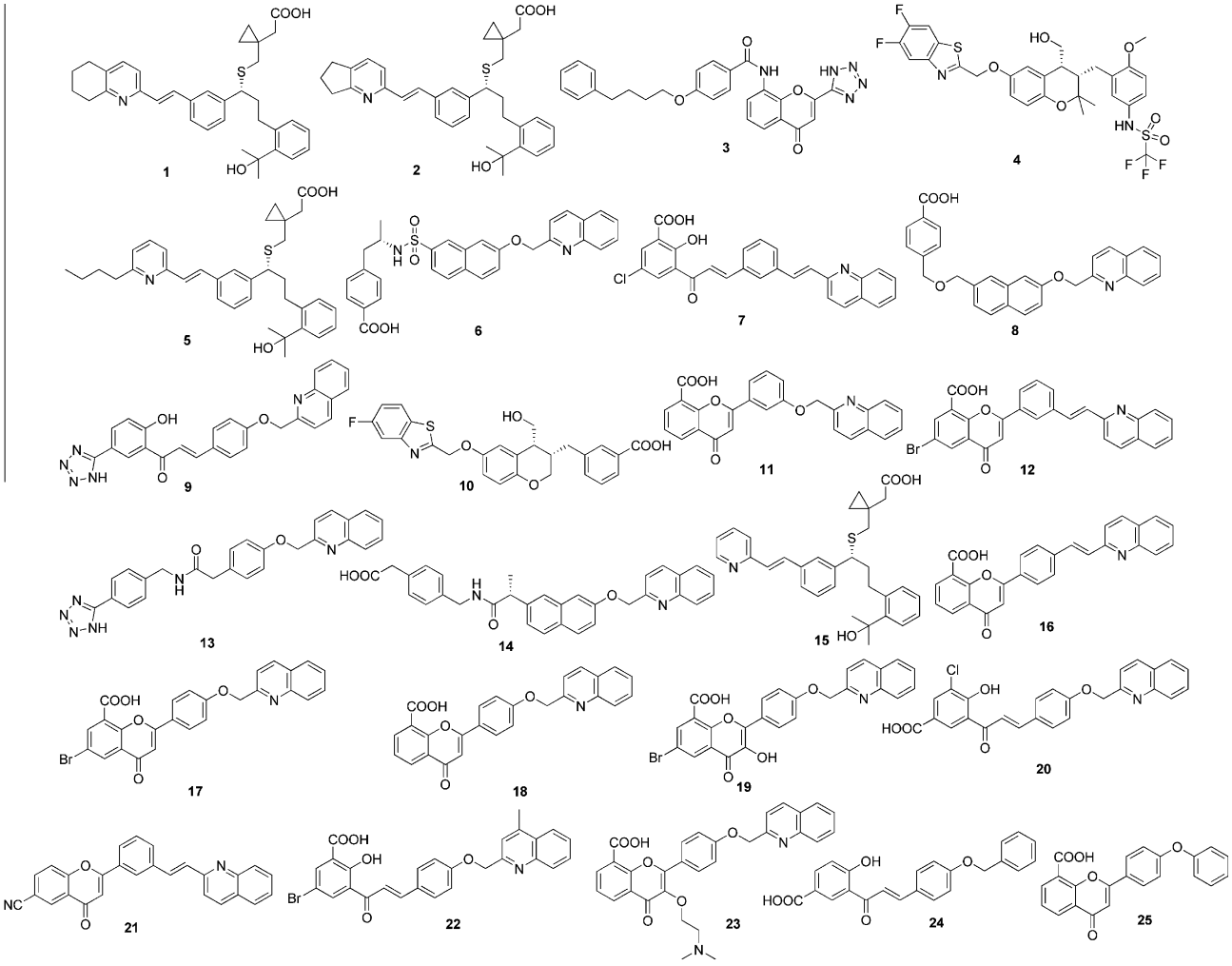


**Figure 2.** 2D chemical structures of the 25 molecules forming the training set used to obtain HypoGen pharmacophore hypotheses.

Chemical Directory (ACD) database (Symyx Technologies, Santa Clara, CA) using 'Random Percent Filter protocol' by Pipeline Pilot software (Accelrys, Inc., San Diego, USA).

Carboxylated chalcone derivatives which were firstly discovered by Zwaagstra et al. and showed preferable $CysLT_1$ antagonistic activities in both in vitro and in vivo assays.[17] These prompted us to design a novel series of carboxylated chalcone derivatives with improved activities. In the course of novel compounds generation program, the effect of different substituents on A-ring of chalcones (e.g., halogen, COOH, hydroxyl) and the influence of different substituent and length of lipophilic chain on B-ring of chalcones (e.g., phenyl or alkyl chain) were taken into consideration. All candidate fragments linked to chalcone skeleton were assembled using Pipeline Pilot student edition (Accelrys, Inc., San Diego, USA).

All compounds were utilized to ascertain the energy-minimized conformations using a CHARMm-like force field.[22] Then, conformational models of each compound were generated using the Poling Algorithm implemented in Catalyst (Catalyst 4.10 documentation). A maximum of 250 conformations were generated for every compound to ensure maximum coverage of the conformational space within an energy threshold of 20.0 kcal/mol.

### 2.2. Pharmacophore generation

Based on the conformations for each compound, the HypoGen algorithm implemented in Catalyst program was employed to establish pharmacophore models. Three chemical feature types termed ring aromatic (AR), hydrophobic (HY) and negative ionizable (NI) features were selected for hypotheses generation, since they could effectively map all critical chemical features of all molecules. All the parameters were set as default and the uncertainty value was set to 3.0 for compound activity, representing the ratio of the uncertainty range of measured biology activity against the actual activity for each compound. The Catalyst program returned 10 pharmacophore models with top ranking scores.

### 2.3. Pharmacophore validation

In order to validate the reliability and accuracy of the generated 3D pharmacophore models, cost analysis, test set activity prediction, Fisher's test and enrichment factors studies were performed.

#### 2.3.1. Cost analysis

The quality of HypoGen models can be described in terms of fixed cost, null cost, and total cost, all of which were well defined by Debnath.[23] As a good model, the total cost of any hypothesis should be close to the fixed cost. If a returned cost (total cost) differs from the null hypothesis by 40–60 bits, it is highly probable that the hypothesis has 75–90% chance representing the true correlation of the data (Catalyst 4.10 documentation).

#### 2.3.2. Test set activity prediction

In addition to estimation of the activity of training set molecules, the pharmacophore model was also used to predict the bioactivities of new compounds. For such a purpose, 52 $CysLT_1$ antagonists in the test set, also having wide range of activities ($IC_{50}$, spanning from 0.21 to 10,500 nM) and structural diversity, were predicted by the best pharmacophore model.

#### 2.3.3. Fisher's test

Using the CatScrambe module, the molecular spreadsheets of our training set were modified by arbitrary scrambling of the affinity data. These randomized spreadsheets should yield hypotheses without statistical significance; otherwise, the original model was also obtained randomly. To achieve a statistical significance level of 95%, 19 random spreadsheets were generated.

#### 2.3.4. Enrichment factor study

In the lead-discovery studies, the pharmacophore model should be useful in identifying active leads in virtual screening. So the generated models were further validated by enrichment factor (EF) studies in screening an database which was retrieved

**Table 1**
Experimental and estimated $CysLT_1$ antagonistic activities of training set based on Hypo1

| Compd | Fit | Mapping | $CysLT_1$ activities($IC_{50}$) | | Error[a] | Activity scale($IC_{50}$) | | |
|---|---|---|---|---|---|---|---|---|
| | | | Exp. (nM) | Est. (nM) | | Exp. | Est. | Ref. |
| **1**[b] | 11.92 | [11 6 36 38 24] | 0.19 | 0.066 | −2.9 | +++ | +++ | 18 |
| **2** | 10.94 | [11 6 36 37 24] | 0.5 | 0.63 | 1.3 | +++ | +++ | 18 |
| **3**[b] | 9.93 | [23 13 10 32 *] | 0.8 | 6.4 | 8 | +++ | +++ | 19 |
| **4** | 9.71 | [5 33 35 * 16] | 2 | 11 | 5.3 | +++ | +++ | 19 |
| **5** | 9.56 | [11 6 * 38 24 ] | 2.4 | 15 | 6.2 | +++ | +++ | 18 |
| **6**[b] | 9.61 | [19 30 31 59 *] | 4.1 | 13 | 3.3 | +++ | +++ | 16 |
| **7** | 9.79 | [2 17 8 49 *] | 6.6 | 9 | 1.4 | +++ | +++ | 17 |
| **8** | 10.19 | [2 15 16 48 *] | 7.3 | 3.6 | −2 | +++ | +++ | 16 |
| **9** | 9.36 | [14 8 1 * 25] | 14 | 24 | 1.7 | ++ | ++ | 19 |
| **10** | 9.67 | [20 1 15 25 *] | 14 | 12 | −1.2 | ++ | ++ | 17 |
| **11**[b] | 9.72 | [14 22 28 30 *] | 17 | 10 | −1.6 | ++ | ++ | 20 |
| **12** | 10.03 | [14 22 28 31 *] | 17 | 5 | −3.4 | ++ | +++ | 21 |
| **13** | 9.48 | [42 13 37 1 *] | 38 | 18 | −2.1 | ++ | ++ | 16 |
| **14**[b] | 8.71 | [57 18 23 * 3] | 130 | 110 | −1.3 | ++ | ++ | 16 |
| **15** | 8.91 | [11 6 * 34 24] | 190 | 68 | −2.9 | ++ | ++ | 18 |
| **16** | 7.75 | [14 22 28 * *] | 270 | 970 | 3.6 | ++ | ++ | 21 |
| **17**[b] | 7.77 | [30 * 27 31 *] | 500 | 920 | 1.8 | ++ | ++ | 21 |
| **18** | 7.76 | [* 22 28 30 *] | 530 | 960 | 1.8 | ++ | ++ | 20 |
| **19**[b] | 7.78 | [2 27 22 * *] | 810 | 910 | 1.1 | ++ | ++ | 20 |
| **20** | 7.67 | [21 * 16 31 *] | 1700 | 1200 | −1.5 | + | + | 17 |
| **21**[b] | 7.80 | [14 22 27 * *] | 1700 | 870 | −2 | + | ++ | 21 |
| **22** | 7.63 | [48 24 31 * *] | 2100 | 1300 | −1.6 | + | + | 17 |
| **23**[b] | 7.78 | [14 28 * 36 *] | 4000 | 910 | −4.4 | + | ++ | 20 |
| **24** | 6.72 | [44 27 * 14 *] | 34,000 | 10,000 | −3.2 | + | + | 17 |
| **25**[b] | 6.23 | [2 14 23 26 *] | 55,000 | 32,000 | −1.7 | + | + | 21 |

[a] Error values is ratio between the estimated and experimental activity, while a negative sign indicates the actual activity is higher than the estimated one.
[b] The compounds were used in enrichment factor studies.

randomly from ACD database (1500 molecules) spiked some known inhibitors (10 molecules, Table 1).

$$\text{Enrichment factor(EF)} = \frac{\text{TP}}{\text{TP}+\text{FP}} \cdot \frac{N}{n},$$

where TP is the number of true positive compounds, FP is the number of false positive compounds, $N$ is the number of the total compounds and $n$ is the number of the total positive compounds.

## 3. Results and discussion

### 3.1. Pharmacophore model development

The results of pharmacophore hypotheses are presented in Table 2. The Hypo1, the best pharmacophore model, describes the topological position of the lipophilic moieties and the acidic residues (Fig. 3A), known as important structural features for $CysLT_1$ receptor antagonists. It is consisted of five features, namely, one ring aromatic (RA), one negative ionizable (NI), three hydrophobic (HY). The total fixed cost of the run is 100.52, the null cost is 200.04, and the total cost of the Hypo1 is 112.74. Then, the cost range between Hypo1 and the fixed cost is 12.22, while that between the null hypothesis and Hypo1 is 77.30 (Table 2), which shows that Hypo1 has more than 90% probability of correlating the data. Noticeably, the total cost of Hypo1 is much closer to the fixed cost than to the null cost. Besides, a high correlation coefficient of 0.956 is observed with RMSD value of 0.901 and the configuration cost of 15.31, demonstrating that a meaningful pharmacophore model with good statistical parameters were successfully developed.

**Table 2**
The results of top 10 hypotheses in HypoGen pharmacophore generation

| Hypo | Total cost | Δcost | RMSD | Correl. |
|---|---|---|---|---|
| 1 | 112.74 | 87.30 | 0.901 | 0.956 |
| 2 | 115.69 | 84.35 | 1.026 | 0.942 |
| 3 | 119.01 | 81.03 | 1.062 | 0.940 |
| 4 | 120.55 | 79.49 | 1.170 | 0.925 |
| 5 | 122.52 | 77.52 | 1.240 | 0.915 |
| 6 | 123.15 | 76.89 | 1.299 | 0.905 |
| 7 | 124.17 | 75.87 | 1.306 | 0.905 |
| 8 | 124.35 | 75.69 | 1.275 | 0.910 |
| 9 | 124.95 | 75.09 | 1.366 | 0.894 |
| 10 | 125.48 | 74.56 | 1.352 | 0.897 |

Null cost of 10 top-scored hypothesis is 200.04, fixed cost value is 100.52, and configuration cost is 15.31.

Table 1 and Fig. 4A represent the actual and estimated $CysLT_1$ antagonistic activities ($IC_{50}$ values) of the 25 training set molecules. Based on their potency of $CysLT_1$ antagonistic activity scale, these 25 compounds were classified to highly active compounds (+++, $IC_{50}$ <10 nM), moderately active compounds (++, 10 nM $\leqslant$ $IC_{50}$ <1000 nM) and weakly active compounds (+, $IC_{50} \geqslant$ 1000 nM). Among the molecules **1–25**, all of highly active compounds were estimated correctly, while only 9.1% of moderately active compounds (compound **12**) and 33.3% of weakly active compounds (compounds **21** and **23**) were predicted wrongly. For example, the $CysLT_1$ antagonistic activities of the most active compound **1** ($IC_{50}$: 0.19 nM) and the weakly active compound **25** ($IC_{50}$: 55,000 nM) could be predicted nicely using Hypo1. In the case of compound **1**, the carboxyl group, aromatic ring and aliphatic chain mapped well onto Hypo1 (fit values: 11.92, Fig. 3B), and the predicted activity fit well with its actual activity (prediction $IC_{50}$: 0.066 nM; actual $IC_{50}$: 0.19 nM). For molecule **25**, three hydrophobic features and carboxyl group could not fit well to corresponding pharmacophore features, and the ring aromatic feature is missed, leading to a poor predicted activity of compound **25** (fit values: 6.23, Fig. 3C), which was also close to its actual activity (prediction $IC_{50}$: 32,000 nM; actual $IC_{50}$: 55,000 nM).

### 3.2. Pharmacophore model validation

#### 3.2.1. Test set prediction

The Hypo1 was further validated by using a test set of 52 compounds which were structurally distinct from those included in the

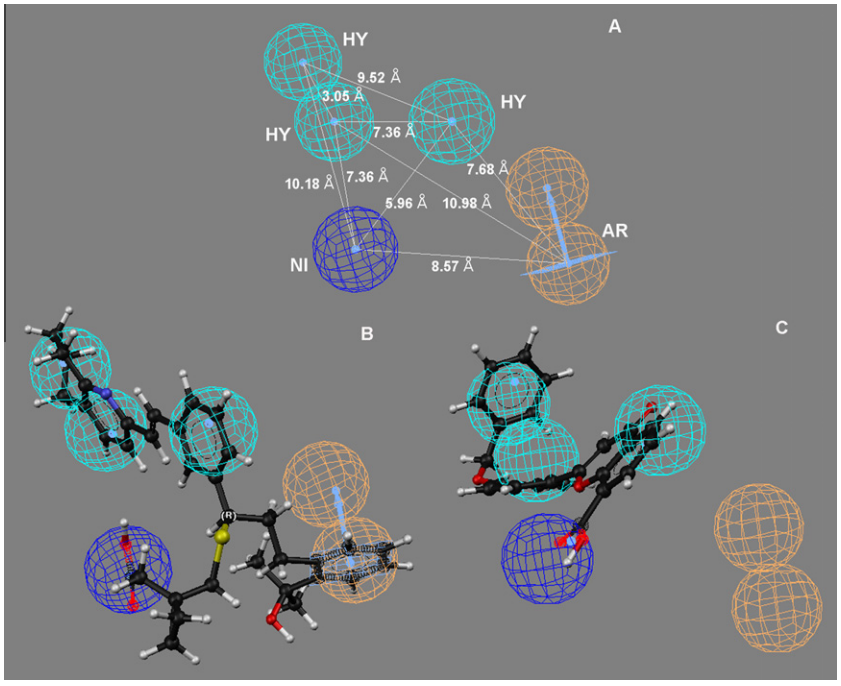


**Figure 3.** The generated best Pharmacophore model (Hypo1) with distance constraints (A); Hypo1 aligned to compound **1** ($K_i$ = 0.19 nM, (B) and **25** ($K_i$ = 55,000 nM, (C). Pharmacophore features are color-coded (hydrophobic, blue; negative ionizable, dark blue; ring aromatic: orange).

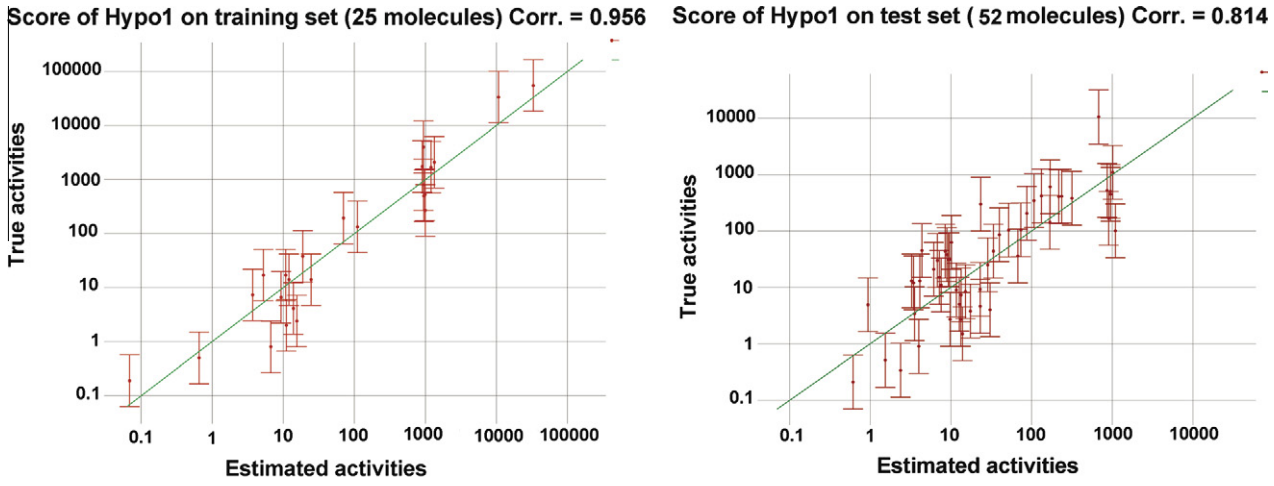


**Figure 4.** The regression line of actual versus predicted activities by Hypo1 for the training set and test set.

training set. The actual activity versus estimated activity of the 52 compounds in the test is shown in Table S1 as the Supplementary data, which showed a good correlation of 0.814 between the actual and the estimated activities (Fig. 4b).

### 3.2.2. Fisher's test

With the aid of the CatScramble program, the experimental activities of compounds in the training set were scrambled randomly, and the resulting training set was used for a HypoGen run. All parameters were adopted and used in the initial HypoGen calculation. This procedure was reiterated 19 times. None of the outcome hypotheses had a lower cost score than the initial hypothesis. Ten lowest total cost values of the resulting 19 hypotheses were compared with our hypothesis costs. None of the costs of the scrambled hypothesis was less than Hypo1 (Fig. 5), indicating that there was a 95% chance for the best hypothesis to represent a true correlation in the training set activity data.

### 3.2.3. Enrichment factor study

The Hypo1 was further validated for picking up active molecules ($CysLT_1$ antagonists) from a database, including 1500 inactive compounds and 10 known inhibitors (labeled in Table 1). The Hypo1 picked up the known inhibitors with highly enrichment factors (18.0, 9.0, 4.5, and 3.3 at 5%, 10%, 20%, and 30%, respectively), indicating that Hypo1 is a useful and reliable tool for identifying $CysLT_1$ antagonists in virtual screening.

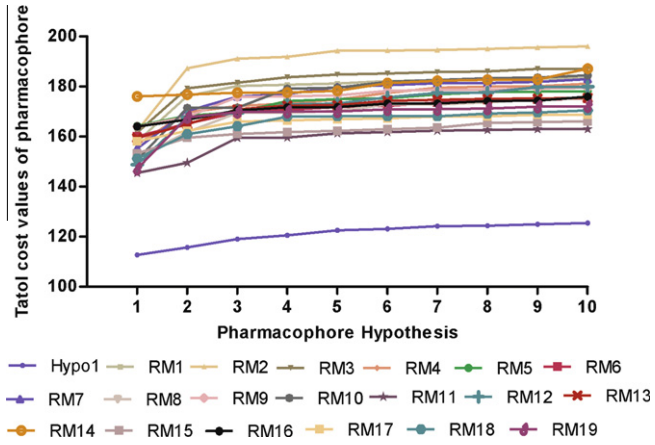


**Figure 5.** The difference in costs between the HypoGen runs (Hypo1) and the scrambled runs (RM1–RM19).

### 3.3. Database searching

To identify novel $CysLT_1$ antagonists, Hypo1 was used as a search query against an in-house databases consisted of carboxylated chalcone derivatives (537 molecules). Interestingly, over ninety compounds fitted well with features of Hypo1 were predicted as potential candidates for further exploration (calcd $K_i$ <300 nM). Then, the synthesis and biological evaluation of four compounds **26a**,**b** and **27a**,**b** (Fig. 6) for their $CysLT_1$ antagonistic activities were performed according to their good prediction activities and synthetic feasibility.

### 3.4. Chemistry

The synthetic route for compounds **26** and **27** is outlined in Scheme 1. Treatment of 4-hydroxybenzaldehyde, appropriate alkylbromide and potassium carbonate in acetone afforded compounds **29**. Claisen–Schmidt condensation of acetophenone **28** with benzaldehyde **29a** in presence of 10% potassium hydroxide in a solvent of EtOH/THF/$H_2O$ (5:5:2) for 2–3 days gave chalcone **31**, which were further etherized with ethyl bromoacetate to yield compounds **32**. Deprotection of the benzoic acid function of **32** using 5% sodium hydroxide in EtOH/$H_2O$ mixture solvent at 40 °C resulted in carboxylated chalcone **26**. Besides, acetophenone **30** were obtained using 4-hydroxybenzoic acid (or 3-hydroxybenzoic acid) as starting materials, according to the literature.[17] Condensation of acetophenone **30** with appropriate benzaldehyde **29** in presence of 10% potassium hydroxide in EtOH/THF/$H_2O$ (5:5:2) mixture solvent for even longer time (5–6 days), following by esterization with ethanol catalyzed by sulfuric acid afforded chalcone **33**. Etherization of **33** with chloroacetonitrile in presence of potassium carbonate in acetone gave in **34**, which were further alkaloid hydrolyzed using 5% sodium hydroxide in EtOH/$H_2O$ mixture solvent at room temperature to get carboxylated chalcone **27**.

### 3.5. $CysLT_1$ antagonistic activities

The in vitro $CysLT_1$ antagonistic potency of the compounds was evaluated in dU937 cells (highly expressing $CysLT_1$ receptor) pre-stimulated by $LTD_4$ according to reported methods.[24–26] In this biological evaluation model, PT-PCR and Western blot analysis showed a higher expression of $CysLT_1$ receptor in dU937 cells. ATP at 50 μmol $L^{-1}$ significantly elevated $[Ca^{2+}]_i$, and was used as a positive control for measurement of $[Ca^{2+}]_i$. $LTD_4$ at 0.1 μmol $L^{-1}$ also significantly increased $[Ca^{2+}]_i$, which could be blocked by Montelukast (a well known $CysLT_1$ antagonist) and compounds

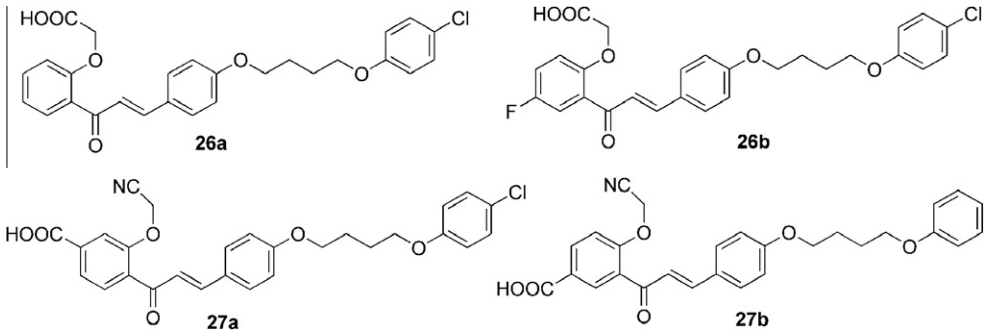


**Figure 6.** The structures of selected carboxylated chalcones **26a**,**b** and **27a**,**b**.

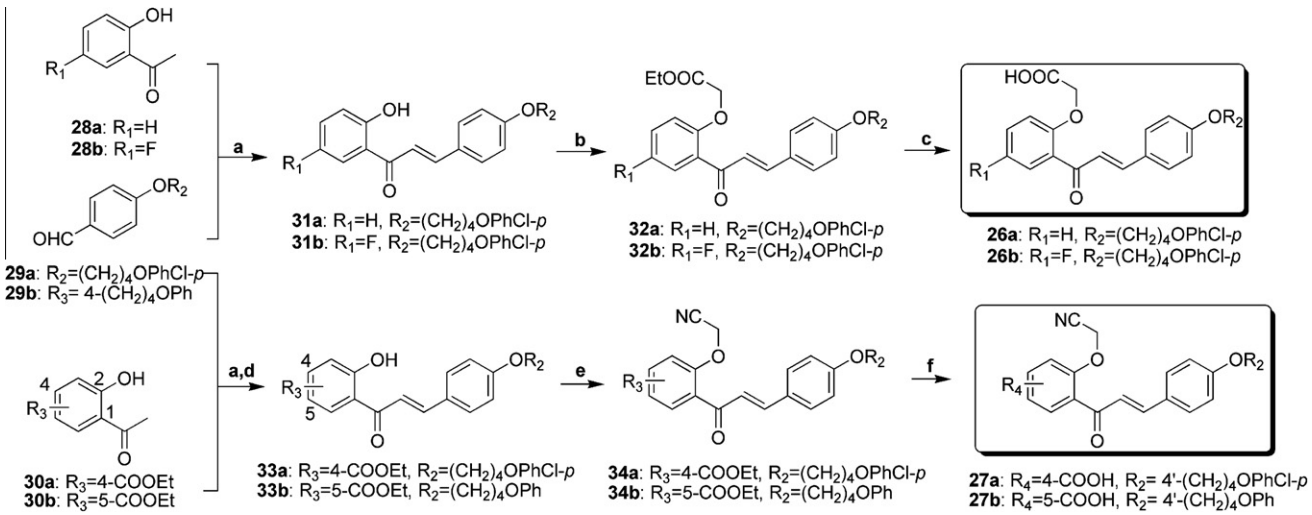


**Scheme 1.** Synthesis of carboxylated chalcones **26a**,**b** and **27a**,**b**. Reagents and conditions: (a) 10% KOH, ethanol/THF/$H_2O$, rt; (b) $BrCH_2COOEt$, $K_2CO_3$, acetone, reflux; (c) 5% NaOH, EtOH/$H_2O$, 40 °C; (d) ethanol, $H_2SO_4$, reflux; (e) $ClCH_2CN$, $K_2CO_3$, acetone, reflux; (f) 5% NaOH, EtOH/$H_2O$, rt.

**26a**,**b** and **27a**,**b**. The promoted antagonistic effects of tested compounds were observed in a dose-dependent manner with the maximal effect observed at 10 μM as shown in Figure 7. The selected four carboxylated chalcones (**26a**,**b** and **27a**,**b**) showed moderate to good $CysLT_1$ antagonistic activities (Table 3), indicating that pharmacophore-based $CysLT_1$ antagonists design was a rational protocol in lead optimization. As expected, the introduction of carboxyl group and lipophilic chain on the A-ring and B-ring of chalcone skeleton, respectively, enhanced the $CysLT_1$ receptor antagonistic activities, which was consisted with what discovered by other groups.[14] Cyanomethoxyl group on A-ring of chalcones may afford additional interaction point, leading to the best antagonistic activities of **27a** ($EC_{50}$ = 0.48 μM), a promising novel lead for further structural optimization and pharmacological studies.

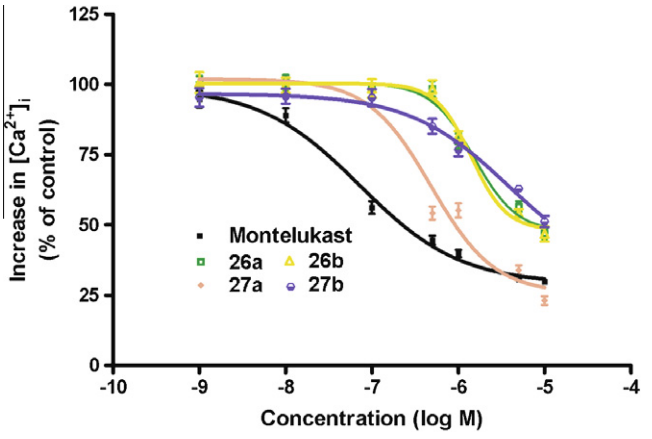


**Figure 7.** The concentration-dependent blocking activity of compounds on $LTD_4$ (0.1 μM)-elevated $[Ca^{2+}]_i$ in dU937 cells curves of some compounds **26a**,**b** and **27a**,**b**.

## 4. Conclusion

In this study, we described a rational strategy for identifying novel $CysLT_1$ antagonists using a pharmacophore-based lead optimization protocol. The best pharmacophore model (Hypo1) was developed using Catalyst/HypoGen program and showed good statistical parameters in validation procedure. Furthermore, four carbonylated chalcones with preferable predictive activities were synthesized and identified as moderate to good $CysLT_1$ antagonists, indicating that pharmacophore-based $CysLT_1$ antagonists design is a rational protocol in lead optimization. To the best of our knowledge, the 3D alignment and pharmacophoric features of $CysLT_1$ antagonists and its application in virtual screening were evaluated for the first time. The most active compound **27a** would be a promising lead for further structural optimization and pharmacological studies.

## 5. Experiment

### 5.1. Chemistry

Melting points were obtained on a B-540 Büchi melting-point apparatus and are uncorrected. $^1H$ NMR spectra was recorded on

**Table 3**
The pharmacological results of synthesized carboxylated chalcones **29a**,**b** and **30a**,**b**

| Compd | Pred. $IC_{50}$[a] (nM) | Exp. $EC_{50}$ (μM) | $E_{max}$ (%) |
|---|---|---|---|
| Montelukast | 5.4 | 0.072 | 70.1 |
| **26a** | 27 | 1.4 | 53.1 |
| **26b** | 87 | 1.3 | 53.2 |
| **27a** | 150 | 0.48 | 76.9 |
| **27b** | 56 | 3.9 | 48.8 |

[a] Predictive $IC_{50}$ value was estimated according to Hypo1.

a 400 MHz spectrometer (Brüker AM), and the chemical shifts were expressed as $\delta$ values in parts per million (ppm) relative to tetramethylsilane (TMS). Mass spectra were recorded on an Esquire-LC-00075 spectrometer. Reagents and solvents were purchased from commercial sources. Acetophenone **28a**,**b** were synthesized according to the literature.[17]

### 5.2. General procedure for the synthesis of benzaldehyde 29a,b

To a stirred solution of 4-hydroxybenzaledhyde and (4-bromobutoxy)benzene (or 1-(4-bromobutoxy)-4-chlorobenzene) in acetone (200 mL), potassium carbonate (11.3 g, 82 mmol) was added. The resulting mixture was refluxed for 5 h, and then cooled to room temperature. The mixture was filtered and the filtrate was concentrated in vacuo. The residue was purified by flash column chromatography on silica gel using petroleum ether/ethyl acetate (10:1, v/v) as eluant to give **29**.

#### 5.2.1. 4-(4-(4-Chlorophenoxy)butoxy)benzaldehyde (29a)

Reagents: 4-hydroxybenzaledhyde (5.0 g, 41.0 mmol), 1-(4-bromobutoxy)-4-chlorobenzene (10.8 g, 41.0 mmol). Product: white solid (9.6 g, 77%), mp 83–85 °C. $^1$H NMR ($CDCl_3$, 400 MHz, $\delta$): 2.01 (m, 4H), 4.03 (t, 2H, $J$ = 6.4 Hz), 4.12 (t, 2H, $J$ = 6.4 Hz), 7.28 (d, 2H, $J$ = 8.0 Hz), 7.54 (d, 2H, $J$ = 8.4 Hz), 7.65 (d, 2H, $J$ = 8.4 Hz), 7.81 (d, 2H, $J$ = 8.0 Hz), 9.83 (s, 1H). ESI-MS: $m/z$ $[M+H]^+$ 305.

#### 5.2.2. 4-(4-Phenoxybutoxy)benzaldehyde (29b)

Reagents: 4-hydroxybenzaldehyde (5.0 g, 41.0 mmol), 4-bromobutoxybenzene (9.3 g, 41.0 mmol). Product: pale yellow syrup (7.5 g, 68%). $^1$H NMR ($CDCl_3$, 400 MHz, $\delta$): 1.99 (m, 4H), 4.01(t, 2H, $J$ = 6.0 Hz), 4.10 (t, 2H, $J$ = 6.0 Hz), 6.88 (m, 3H), 7.03 (d, 2H, $J$ = 8.0 Hz),7.22 (t, 2H, $J$ = 8.0), 7.68 (d, 2H, $J$ = 8.0 Hz), 9.82 (s, 1H). ESI-MS: $m/z$ $[M+H]^+$ 271.

### 5.3. General procedure for the synthesis of chalcone 31a,b

A solution of acetophenone **28**, benzaldehyde **29a**, and 10% potassium hydroxide in a solvent of EtOH/THF/$H_2O$ (5:5:2, v/v, 6 mL) was stirred at room temperature for 2–3 days. The reaction mixture was poured into ice-water, acidified to pH ~5 with 2 N HCl and extracted with ethyl acetate (20 mL × three times). The organic phase was washed with brine, dried over anhydrous $Na_2SO_4$, and then concentrated in vacuo. The residue was purified by column chromatography on silica gel using petroleum ether/ethyl acetate (15:1, v/v) as eluant to give **31**.

#### 5.3.1. (*E*)-3-(4-(4-(4-Chlorophenoxy)butoxy)phenyl)-1-(2-hydroxyphenyl)prop-2-en-1-one (31a)

Reagents: acetophenone **28a** (500 mg, 3.68 mmol) and benzaldehyde **29a** (1.17 g, 3.86 mmol). Product: pale yellow solid (1.01 g, 65%), mp 125–128 °C. $^1$H NMR ($CDCl_3$, 400 MHz, $\delta$): 1.99 (m, 4H), 4.01(m, 2H), 4.10 (m, 2H), 6.81 (d, 2H, $J$ = 8.0 Hz), 6.93 (d, 2H, $J$ = 8.0 Hz), 7.03 (td, 1H, $J$ = 1.6, 7.6 Hz), 7.21 (d, 2H, $J$ = 8.0 Hz), 7.47 (t, 2H, $J$ = 7.6 Hz), 7.55 (d, 1H, $J$ = 16.0 Hz), 7.63 (d, 2H, $J$ = 8.0 Hz), 7.89 (d, 1H, $J$ = 16.0 Hz), 7.92 (d, 1H, $J$ = 7.6 Hz), 12.64 (s, 1H, OH). ESI-MS: $m/z$ $[M+H]^+$ 423.

#### 5.3.2. (*E*)-1-(4-Fluoro-2-hydroxyphenyl)-3-(4-(4-phenoxybutoxy)phenyl)prop-2-en-1-one (31b)

Reagents: acetophenone **28b** (500 mg, 3.25 mmol), benzaldehyde **29a** (1.04 g, 3.41 mmol). Product: pale yellow solid (0.83 g, 58%), mp 137–139 °C. $^1$H NMR ($CDCl_3$, 400 MHz, $\delta$): 1.94 (m, 4H), 4.03(m, 2H), 4.12 (m, 2H), 6.84 (d, 2H, $J$ = 8.0 Hz), 6.96 (d, 2H, $J$ = 8.0 Hz), 7.03 (dd, 1H, $J$ = 5.2, 7.6 Hz), 7.22 (d, 2H, $J$ = 8.0 Hz), 7.26 (td, $J$ = 8.0, 1.2 Hz, 1H),7.32 (dd, $J$ = 8.0, 1H, 1.2 Hz), 7.54 (d, 1H, $J$ = 16.0 Hz), 7.80 (d, 2H, $J$ = 8.0 Hz), 7.92 (d, 1H, $J$ = 16.0 Hz), 12.64 (s, 1H, OH). ESI-MS: $m/z$ $[M+H]^+$ 441.

### 5.4. General procedure for the synthesis of compounds 32a,b

To a solution of compound **31** and ethyl bromoacetate in acetone (20 mL), potassium carbonate (325.7 mg, 2.36 mmol) was added. The resulting mixture was refluxed for 5 h and then cooled to room temperature. The mixture was filtered and the filtrate was concentrated in vacuo. The residue was purified by flash column chromatography on silica gel using petroleum ether/ethyl acetate (10:1, v/v) as eluant to give **32**.

#### 5.4.1. (*E*)-Ethyl 2-(2-(3-(4-(4-(4-chlorophenoxy)butoxy)phenyl) acryloyl)phenoxy)acetate (32a)

Reagents: compound **31a** (500 mg, 1.18 mmol) and ethyl bromoacetate (198 mg, 1.18 mmol). Product: pale yellow solid (493 mg, 82%), mp: 103–105 °C. $^1$H NMR ($CDCl_3$, 400 MHz, $\delta$): 1.27 (t, 3H, $J$ = 6.0 Hz), 1.97 (m, 4H), 4.00 (m, 2H), 4.06 (m, 2H), 4.65 (s, 2H), 6.80 (d, 2H, $J$ = 8.4 Hz), 6.89 (d, 2H, $J$ = 8.4 Hz), 7.21 (d, 2H, $J$ = 8.4 Hz), 7.36 (m, 2H), 7.37 (d, 1H, $J$ = 16.4 Hz), 7.56 (d, 2H, $J$ = 8.4 Hz), 7.72 (d, 1H, $J$ = 1.2 Hz), 7.98 (d, 1H, $J$ = 16.4 Hz). ESI-MS: $m/z$ $[M+H]^+$ 509.

#### 5.4.2. (*E*)-Ethyl 2-(2-(3-(4-(4-(4-chlorophenoxy)butoxy)phenyl) acryloyl)-5-fluorophenoxy)acetate (32b)

Reagents: compound **31b** (500 mg, 1.14 mmol) and ethyl bromoacetate (190 mg, 1.14 mmol). Product: pale yellow solid (526 mg, 88%), mp: 115–118 °C. $^1$H NMR ($CDCl_3$, 400 MHz, $\delta$):1.25 (t, 3H, $J$ = 6.0 Hz), 1.94 (m, 4H), 4.02 (m, 2H), 4.05 (m, 2H), 4.65 (s, 2H), 6.95 (d, 2H, $J$ = 8.0 Hz), 7.00 (dd, 1H, $J$ = 4.0, 8.0 Hz), 7.12 (d, 2H, $J$ = 8.0 Hz), 7.21 (d, 2H, $J$ = 8.0 Hz), 7.36 (m, 1H), 7.40 (dd, 1H, $J$ = 2.0, 8.0 Hz), 7.37 (d, 1H, $J$ = 16.4 Hz), 7.67 (d, 2H, $J$ = 8.4 Hz), 7.98 (d, 1H, $J$ = 16.4 Hz) ESI-MS: $m/z$ $[M+H]^+$ 527.

### 5.5. General procedure for the synthesis of compounds 26a,b

A solution of **32** and 5% sodium hydroxide in EtOH/$H_2O$ (1:1, v/v, 2 mL) was stirred at 40 °C for 3 h, then poured into cold water and extracted with ethyl acetate (10 mL × three times). The organic phase was washed with brine, dried over anhydrous $Na_2SO_4$, and then concentrated in vacuo. The crude product was recrystallized in ethanol to give expected compound.

#### 5.5.1. (*E*)-2-(2-(3-(4-(4-(4-Chlorophenoxy)butoxy)phenyl)acryloyl)phenoxy)acetic acid (26a)

Reagents: compound **32a** (50 mg, 0.1 mmol). Product: pale yellow solid (35.4 mg, 75%), mp 132–134 °C. $^1$H NMR (acetone-$d_6$, 400 M, $\delta$): 1.93 (m, 4H), 4.04 (t, 2H, $J$ = 6.4 Hz), 4.11 (t, 2H, $J$ = 6.4 Hz), 4.87 (s, 2H), 6.90 (d, 2H, $J$ = 8.8 Hz), 6.93 (d, 2H, $J$ = 8.8 Hz), 7.05 (td, 1H, $J$ = 1.6, 8.4 Hz), 7.11 (d, 1H, $J$ = 8.4 Hz), 7.23 (d, 2H, $J$ = 8.8 Hz), 7.47 (td, 2H, $J$ = 1.6, 8.4 Hz), 7.58 (d, 1H, $J$ = 16.0 Hz), 7.60 (d, 1H, $J$ = 8.4 Hz), 7.63 (d, 1H, $J$ = 16.0 Hz), 7.67 (d, 2H, $J$ = 8.8 Hz). ESI-MS: $m/z$ $[M-H]^-$ 479.

#### 5.5.2. (*E*)-2-(2-(3-(4-(4-(4-Chlorophenoxy)butoxy)phenyl)acryloyl)-5-fluorophenoxy)acetic acid (26b)

Reagent: compound **32b** (50 mg, 0.095 mmol). Product: pale yellow solid (32.2 mg, 68%), mp 122–124 °C?$^1$H NMR (acetone-$d_6$, 400 M, $\delta$): 1.98 (m, 4H), 4.09 (t, 2H, $J$ = 6.4 Hz), 4.16 (t, 2H, $J$ = 6.4 Hz), 4.91 (s, 2H), 6.96 (d, 2H, $J$ = 8.4 Hz), 6.98 (d, 2H, $J$ = 8.0 Hz), 7.21 (dd, 1H, $J$ = 4.0, 8.8 Hz), 7.28 (d, 2H, $J$ = 8.4 Hz), 7.29 (m, 1H), 7.38 (dd, 1H, $J$ = 3.2, 8.8 Hz), 7.65 (d, 1H, $J$ = 16.0 Hz), 7.68 (d, 1H, $J$ = 16.0 Hz), 7.72 (d, 2H, $J$ = 8.0 Hz). ESI-MS: $m/z$ $[M-H]^-$ 497.

### 5.6. General procedure for the synthesis of compounds 33a,b

A solution of acetophenone **30**, corresponding benzaldehyde **29**, and 10% potassium hydroxide in a solvent of EtOH/THF/$H_2O$ (5:5:1, v/v, 6 mL) was stirred at room temperature for 5–6 days. The mixture was poured into ice-water, acidified to pH ~5 with 2 N HCl, and extracted with ethyl acetate (20 mL × three times). The organic phase was washed with brine, dried over anhydrous $Na_2SO_4$, and then concentrated in vacuo to give pale yellow syrup, to which ethanol (10 mL) and sulfuric acid (two drops) was added. The reaction mixture was refluxed for 4 h. Upon finishing of the reaction, water was added, and the mixture was extracted with ethyl acetate (20 mL × three times), then washed with brine and dried over anhydrous $Na_2SO_4$. Evaporating of the combined organic layers afforded the crude product as an oily residue which was purified by flash column chromatography on silica gel using petroleum ether/ethyl acetate (8:1, v/v) as eluant to give **33**.

#### 5.6.1. (*E*)-Ethyl 4-(3-(4-(4-(4-chlorophenoxy)butoxy)phenyl) acryloyl)-3-hydroxybenzoate (33a)

Reagent: acetophenone **30a** (500 mg, 2.4 mmol) and benzaldehyde **29a** (768 mg, 2.52 mmol). Product: pale yellow syrup (380 mg, 32%). $^1$H NMR ($CDCl_3$, 400 MHz, $\delta$): $^1$H NMR ($CDCl_3$, 400 MHz, $\delta$): 1.26 (t, 3H, $J$ = 6.0 Hz), 2.01 (m, 4H), 4.00 (t, 2H, $J$ = 6.0 Hz), 4.02 (t, 2H, $J$ = 6.0 Hz), 4.11 (q, 2H, $J$ = 6.0 Hz), 6.89 (d, 2H, $J$ = 8.0 Hz), 6.93 (d, 2H, $J$ = 8.8 Hz), 7.23 (d, 2H, $J$ = 8.0 Hz), 7.52 (d, 1H, $J$ = 16.0 Hz), 7.56 (dd, 1H, $J$ = 1.2, 7.6 Hz), 7.64 (d, 2H, $J$ = 8.8 Hz), 7.67 (d, 1H, $J$ = 7.6 Hz), 7.93 (d, 1H, $J$ = 16.0 Hz), 7.98 (d, 1H, $J$ = 1.2 Hz), 12.65 (s, 1H, OH). ESI-MS: $m/z$ $[M+H]^+$ 495.

#### 5.6.2. (*E*)-Ethyl 4-hydroxy-3-(3-(4-(4-phenoxybutoxy)phenyl) acryloyl)benzoate (33b)

Reagent: acetophenone **30b** (500 mg, 2.40 mmol), benzaldehyde **29b** (681 mg, 2.52 mmol). Product: pale yellow syrup (331 mg, 30%). $^1$H NMR ($CDCl_3$, 400 MHz, $\delta$): 1.28 (t, 3H, $J$ = 6.0 Hz), 2.01 (m, 4H), 4.02 (t, 2H, $J$ = 6.0 Hz), 4.04 (t, 2H, $J$ = 6.0 Hz), 4.11 (q, 2H, $J$ = 6.0 Hz), 6.93 (d, 2H, $J$ = 8.0 Hz), 6.95 (m, 3H), 7.05 (d, 1H, $J$ = 8.0 Hz), 7.26 (d, 2H, $J$ = 8.0 Hz), 7.62 (d, 1H, $J$ = 16.0 Hz), 7.64 (d, 2H, $J$ = 8.0 Hz), 7.95 (d, 1H, $J$ = 16.0 Hz), 8.11 (dd, 1H, $J$ = 1.2, 8.0 Hz), 8.63 (d, 1H, $J$ = 1.2 Hz), 12.68 (s, 1H, OH). ESI-MS: $m/z$ $[M+H]^+$ 461.

### 5.7. General procedure for the synthesis of compounds 27a,b

To a solution of compound **33** and chloroacetonitrile in acetone (20 mL), potassium carbonate was added. The resulting mixture was refluxed for 5 h and then cooled to room temperature. The mixture was filtered and the filtrate was concentrated in vacuo to give **34**. And then 5% sodium hydroxide in EtOH/$H_2O$ (1:1, v/v, 2 mL) was added to the residue. The reaction mixture was stirred at room temperature for 5 h, then poured into cold water and extracted with ethyl acetate. The organic phase was washed with brine, dried over anhydrous $Na_2SO_4$, and then concentrated in vacuo. The crude product was recrystallized in ethanol to give **27**.

#### 5.7.1. (*E*)-4-(3-(4-(4-(4-Chlorophenoxy)butoxy)phenyl)acryloyl)-3-(cyanomethoxy)benzoic acid (27a)

Reagent: compound **36a** (100 mg, 0.20 mmol), chloroacetonitrile (15.3 mg, 0.20 mmol), potassium carbonate (55.9 mg, 0.41 mmol). Product: pale yellow solid (56.2 mg, 55%), mp 148–151 °C. $^1$H NMR (DMSO-$d_6$, $\delta$): 1.94 (m, 4H), 4.04 (t, 2H, $J$ = 6.0 Hz), 4.11 (t, 2H, $J$ = 6.0 Hz), 4.96 (s, 2H), 6.91 (d, 2H, $J$ = 8.8 Hz), 6.95 (d, 2H, $J$ = 8.4 Hz), 7.23 (d, 2H, $J$ = 8.8 Hz), 7.44 (d, 1H, $J$ = 16.0 Hz), 7.56 (d, 1H, $J$ = 16.0 Hz), 7.59 (d, 1H, $J$ = 8.0 Hz), 7.60 (s, 1H), 7.66 (d, 2H, $J$ = 8.4 Hz), 7.72 (d, 1H, $J$ = 1.6, 8.0 Hz). ESI-MS: $m/z$ $[M-H]^-$ 504.

#### 5.7.2. (*E*)-4-(Cyanomethoxy)-3-(3-(4-(4-phenoxybutoxy)phenyl) acryloyl)benzoic acid (27b)

Reagent: compound **36b** (100 mg, 0.22 mmol), chloroacetonitrile (16.4 mg, 0.22 mmol), potassium carbonate (60 mg, 0.44 mmol). Product: pale yellow solid (49.1 mg, 48%), mp 173–176 °C. $^1$H NMR (DMSO-$d_6$, $\delta$): 1.92 (m, 4H), 4.03 (t, 2H, $J$ = 6.0 Hz), 4.10 (t, 2H, $J$ = 6.0 Hz), 4.96 (s, 2H), 6.86 (t, 1H, $J$ = 8.8 Hz), 6.95 (d, 2H, $J$ = 8.4 Hz), 6.98 (d, 2H, $J$ = 8.0 Hz), 7.22 (d, 1H, $J$ = 8.4 Hz), 7.30 (t, 2H, $J$ = 8.8 Hz), 7.56 (d, 1H, $J$ = 16.0 Hz), 7.59 (d, 1H, $J$ = 16.0 Hz), 7.69 (d, 2H, $J$ = 8.4 Hz), 8.05 (dd, 1H, $J$ = 2.0, 8.4 Hz), 8.08 (d, 1H, $J$ = 8.4 Hz). ESI-MS: $m/z$ $[M-H]^-$ 470.

### 5.8. Pharmacological evaluation of $CysLT_1$ antagonistic activities

#### 5.8.1. Materials

RPMI 1640 was purchased from Grand Island Biological Company (Gibco, USA). Fetal bovine serum was purchased from Shanghai Genetimes Technology, Inc. (China), and penicillin, streptomycin, L-glutamine and pluronic F-127 were purchased from Invitrogen Co. (USA). $LTD_4$, Fluo3/AM, dimethylsulfoxide, and Hepes were purchased from Sigma Chem. Co (USA). All salts for saline and Tris solution were purchased from Shanghai Sangon Biological Engineering Technology and Services Co., Ltd (China). Disposable culture flasks, petri dishes, and filters were purchased from Corning Glass Works (USA). Montelukast was a kind gift from Merck & Co., Inc. (USA).

#### 5.8.2. Cell culture

U937 cells (ATCC) were routinely cultured into flasks in RPMI 1640 medium supplemented with 10% fetal bovine serum, 2 mM L-glutamine, 4.5 g/L D-glucose, 10 mM Hepes, 2 g/L $NaHCO_3$, 1 mM sodium pyruvate, 100 U/mL penicillin, and 100 mg/mL streptomycin at 37 °C (5% $CO_2$) and differentiated for 4–5 days with 1.3% dimethyl sulfoxide (DMSO).

#### 5.8.3. Determination of cytosolic free $Ca^{2+}$ levels

Briefly, dU937 Cells were washed twice with a balanced salt solution (BSS in mM: NaCl 140, KCl 4, $MgCl_2$ 1, $CaCl_2$ 1.25, HEPES 5, glucose 11, $NaH_2PO_4$ 1, ascorbic acid 5.7; pH 7.4) and incubated in 1 mL BSS containing 10 μM Fluo3/AM and 0.03% pluronic F-127 for 45 min at 37 °C. After loading, Fluo3/AM was removed and cells were washed twice with BSS. Then, cells were centrifuged, resuspended, diluted to the concentration of $10^6$ cells/mL, and transferred to 96 wells plate. Tested compounds were added to the wells with 10 μL at the different concentration and were further incubated for 30 min at 37 °C to complete the hydrolysis of Fluo3/AM. Cells were transferred to the FLUOstar OPTIMA (BMG Germany) and $LTD_4$ was added to the wells at the concentration of 0.1 μM. Calcium concentration ($[Ca^{2+}]_i$) were measured as the fluorescence monitored at 37 °C (485 nm excitation, 525 nm emission). The half maximum antagonistic concentration ($EC_{50}$) was defined as the concentration of the compounds that induced 50% of

maximum inhibition of $[Ca^{2+}]_i$ elevated by $LTD_4$ (0.1 μM) and was calculated from the concentration–response curve by nonlinear regression (curve fit) using GraphPad Prism (Version 4.0).

## Acknowledgments

This study was financially supported by the National Natural Science Foundation of China (No. 30772561) and the National Key Tech Project for Major Creation of New drugs (No. 2009ZX09501-003).

## Supplementary data

Supplementary data associated with this article can be found, in the online version, at doi:10.1016/j.bmc.2010.06.047.

## References and notes

1. Claesson, H. E.; Dahlen, S. E. *J. Int. Med.* **1999**, *245*, 205.
2. Samuelsson, B.; Dahlen, S. E.; Lindgren, J. A.; Rouzer, C.; Serhan, C. N. *Science* **1987**, *237*, 1171.
3. Lieberman, P. *Allergy Asthma Proc.* **2009**, *30*, 345.
4. Folco, G.; Rossoni, G.; Buccellati, C.; Berti, F.; Maclouf, J.; Sala, A. *Am. J. Respir. Crit. Care Med.* **2000**, *161*, S112.
5. Sampson, A. P.; Pizzichini, E.; Bisgaard, H. *J. Allergy. Clin. Immunol.* **2003**, *111*, S49. discussion S59–61.
6. Pergola, C.; Werz, O. *Expert Opin. Ther. Patents* **2010**, *20*, 355.
7. Coleman, R. A.; Eglen, R. M.; Jones, R. L.; Narumiya, S.; Shimizu, T.; Smith, W. L. *Adv. Prostaglandin Thromboxane Leukot. Res.* **1995**, *23*, 283.
8. Metters, K. M.; Gareau, Y.; Lord, A.; Rochette, C.; Sawyer, N. J. *J. Pharmacol. Exp. Ther.* **1994**, *270*, 399.
9. Hamilton, A.; Faiferman, I.; Stober, P.; Watson, R. M.; O'Byrne, P. M. *J. Allergy Clin. Immunol.* **1998**, *102*, 177.
10. Markham, A.; Faulds, D. *Drugs* **1998**, *56*, 251.
11. Jacobs, R. T.; Brown, F. J.; Cronk, L. A.; Aharony, D.; Buckner, C. K.; Kusner, E. J.; Kirkland, K. M.; Neilson, K. L. *J. Med. Chem.* **1993**, *36*, 394.
12. Yu, G. L.; Wei, E. Q.; Wang, M. L.; Zhang, W. P.; Zhang, S. H.; Weng, J. Q.; Chu, L. S.; Fang, S. H.; Zhou, Y.; Chen, Z.; Zhang, Q.; Zhang, L. H. *Brain Res.* **2005**, *1053*, 116.
13. Labelle, M.; Belley, M.; Gareau, Y.; Gauthier, J. Y.; Guay, D.; Gordon, R.; Grossman, S. G.; Jones, T. R.; Leblanc, Y.; McAuliffe, M.; McFarlane, C.; Masson, P.; Metters, K. M.; Ouimet, N.; Patrick, D. H.; Piechuta, H.; Rochette, C.; Sawyer, N.; Xiang, Y. B.; Pickett, C. B.; Ford-Hutchinson, A. W.; Zamboni, R. J.; Young, R. N. *Bioorg. Med. Chem. Lett.* **1995**, *5*, 283.
14. Zwaagstra, M. E.; Schoenmakers, S. H. H. F.; Nederkoorn, P. H. J.; Gelens, E.; Timmerman, H.; Zhang, M. *J. Med. Chem.* **1998**, *41*, 1439.
15. *QSAR and Drug Design-New Developments and Applications*; Terada, H., Goto, S., Hori, H., Taira, Z., Fujita, T., Eds.; Elsevier: Amsterdam, 1995. pp 341–367.
16. Palomer, A.; Pascual, J.; Cabre, F.; Garcia, M. L.; Mauleon, D. *J. Med. Chem.* **2000**, *43*, 392.
17. Zwaagstra, M. E.; Timmerman, H.; Tamura, M.; Tohma, T.; Wada, Y.; Onagi, K.; Zhang, M. *J. Med. Chem.* **1997**, *40*, 1075.
18. Guay, D.; Gauthier, J. Y.; Dufresne, C.; Jones, T. R.; McAuliffe, M.; MacFarlane, C.; Metters, K. M.; Prasit, P.; Rochette, C.; Roy, P.; Sawyer, N.; Zamboni, R. *Bioorg. Med. Chem. Lett.* **1998**, *8*, 453.
19. Zwaagstra, M. E.; Timmerman, H.; Abdoelgafoer, R. S.; Zhang, M. *Eur. J. Med. Chem.* **1996**, *31*, 861.
20. Zwaagstra, M. E.; Korthouwer, R. E. M.; Timmerman, H.; Zhang, M. *Eur. J. Med. Chem.* **1998**, *33*, 95.
21. Zwaagstra, M. E.; Timmerman, H.; Stolpe, A. C.; Kanter, F. J. J.; Tamura, M.; Wada, Y.; Zhang, M. *J. Med. Chem.* **1998**, *41*, 1428.
22. Weiner, S. J.; Kollman, P. A.; Ngyuen, D. T.; Case, D. A. *J. Comput. Chem.* **1986**, *7*, 230.
23. Debnath, A. K. *J. Med. Chem.* **2002**, *45*, 41.
24. Capra, V.; Ravasi, S.; Accomazzo, M. R.; Parenti, M.; Rovati, G. E. *Biochem. Pharmacol.* **2004**, *67*, 1569.
25. Frey, E. A.; Nicholson, D. W.; Metters, K. M. *Eur. J. Mol. Pharmacol.* **1993**, *244*, 239.
26. Capra, V.; Accomazzo, M. R.; Ravasi, S.; Parenti, M.; Macchia, M.; Nicosia, S.; Rovati, G. E. *Prostaglandins Other Lipid Mediat* **2003**, *71*, 235.